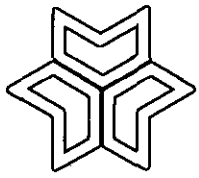

Fluids and Hydraulics

MODELING CONTAMINATION OF SHALLOW UNCONFINED AQUIFERS THROUGH INFILTRATION BEDS

David W. Ostendorf

Water Resources Research

In Press, 1985 3

Department of Civil Engineering
University of Massachusetts at Amherst

MODELING CONTAMINATION OF SHALLOW UNCONFINED AQUIFERS THROUGH INFILTRATION BEDS

David W. Ostendorf

Water Resources Research

In Press, 1985 3

WRR, VOL. 22, PP. 375-382 (1986)

ABSTRACT

We model the transport of a simply reactive contaminant through an infiltration bed and underlying shallow, one dimensional, unconfined aquifer with a plane, steeply sloping bottom in the assumed absence of dispersion and downgradient dilution. The effluent discharge and ambient groundwater flow under the infiltration beds are presumed to form a vertically mixed plume marked by an appreciable radial velocity component in the near field flow region. The near field analysis routes effluent contamination as a single linear reservoir whose output forms a source plane for the one dimensional, far field flow region downgradient of the facility; the location and width of the source plane reflect the relative strengths of ambient flow and effluent discharge. We model far field contaminant transport using an existing method of characteristics solution with frame speeds modified by recharge, bottom slope, and linear adsorption, and concentrations reflecting first order reaction kinetics. The near and far field models simulate transport of synthetic detergents, chloride, total nitrogen, and boron in a contaminant plume at the Otis Air Force Base sewage treatment plant in Barnstable County, Massachusetts with reasonable accuracy.

INTRODUCTION

We model the transport of a simply reactive contaminant through an infiltration bed and underlying shallow, one dimensional, unconfined aquifer with a plane, steeply sloping bottom in the assumed absence of dispersion and downgradient dilution. The resulting quantitative understanding of the physical transport mechanisms and time scales associated with unconfined aquifer pollution can enable us to identify the source history of existing plumes and predict trajectories of future contamination. This appreciation is prerequisite for the assessment of the emerging evidence of subsurface water pollution from infiltration beds receiving industrial [Pinder, 1973], municipal [LeBlanc, 1984], and domestic [Childs et al., 1974] wastewater flows. Proper regulation, design, and operation of future facilities necessitates quantitative tools as well.

Infiltration beds alter the natural hydraulics by introducing a locally significant amount of water to the subsurface flow field and, in this regard, differ from landfills and other solid waste disposal mechanisms as a source of subsurface pollution. Analytical and numerical models have been used to describe water and contaminant transport induced by artificial infiltration. The classical analysis of Hantush [1967] investigates the transient groundwater mound of finite height forming under a rectangular or circular infiltration bed for a flat ambient water table. The resulting analytical solution is a somewhat unwieldy sum of tabulated functions, so that Finnemore and Hantzsche [1983] propose a curve-fit approximation, valid for long time intervals. Hanson and Brock [1984] incorporate the effect of a sloping water table on mound hydraulics for a strip source of infiltration, using a numerical finite different model. The coupled phenomenon of contaminant transport adds another degree of complexity to the

problem, necessitating a numerical approach for this modeling effort as well. Bedient et al. [1983] modify an existing finite difference code to simulate contaminant transport under infiltration beds for a municipal sewage treatment plant, while Pinder [1973] pursues a finite element analysis of the chromium plume downgradient of an industrial disposal pond.

The numerical models, with their attendant documentation requirements, are appropriate for detailed studies of well instrumented plumes in aquifers of complex geometry; a simple analytical approach is appropriate however, for the preliminary analysis of sparsely measured contamination in an aquifer of simple geometry. We pursue the latter method by extending an existing analysis of landfill leachate migration through mildly sloping aquifers [Ostendorf et al., 1984] to account for artificial infiltration and a steeply sloping underlying aquiclude. Ostendorf et al. [1984] apply the near field-far field schematization commonly used by surface water quality modelers [Fischer et al., 1979] to the groundwater environment. The near field under the landfill routes pollution input as a linear reservoir [Gelhar and Wilson, 1974] whose vertically mixed output forms the far field source term at the downgradient edge of the facility. Ostendorf et al. [1984] analyze the advective transport in the latter region with a method of characteristics solution with frame speeds modified by second order recharge, head loss, and bottom slope effects.

FAR FIELD ANALYSIS

The steady conservation of water mass in a one dimensional, unconfined aquifer subject to strong natural recharge ϵ is

$$q = q_s + \epsilon(x-x_s) \qquad (1)$$

with distance x downgradient of the pollutant source, where conditions are denoted by an s subscript, as indicated in Figure 1. The discharge q per

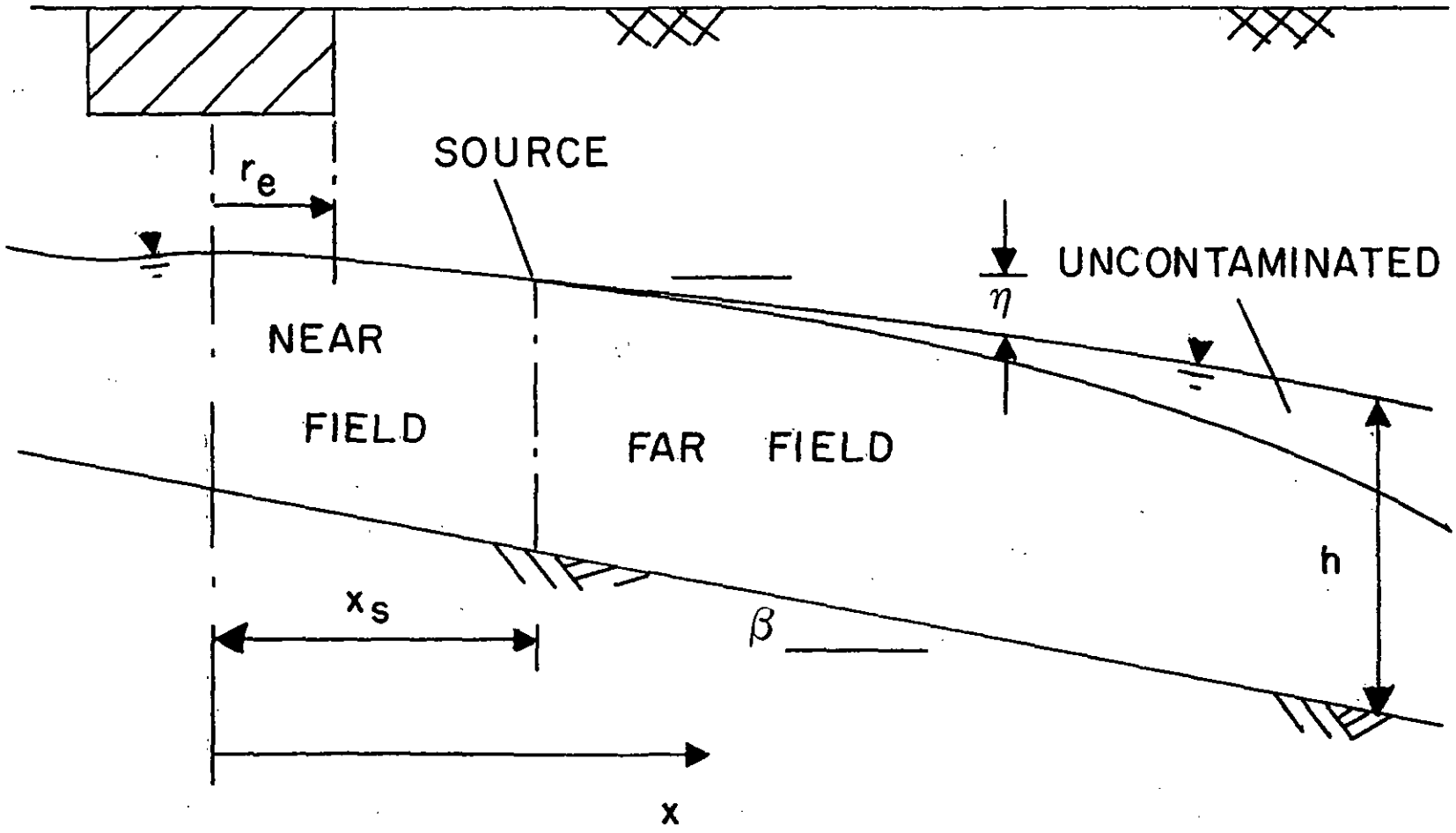

FIGURE 1. DEFINITION SKETCH.

unit width and average linear velocity u in the x direction are related by definition

$$u = \frac{q}{nh} \tag{2}$$

with porosity n and aquifer thickness h given by

$$h = h_s + (x-x_s)\tan\beta - \eta \tag{3}$$

We assume a steeply inclined bottom of slope $\tan\beta$ so that the depression η of the water table below its source position is negligibly small

$$h_s + (x-x_s)\tan\beta >> \eta \tag{4}$$

and, to leading order, equations 1-3 specify the far field average linear velocity

$$u = u_s \left[\frac{1 + \frac{\varepsilon(x-x_s)}{q_s}}{1 + \frac{(x-x_s)\tan\beta}{h_s}} \right] \tag{5}$$

In contrast to the analysis of Ostendorf et al. [1984], natural recharge and bottom slope are assumed to exhibit first order behavior in equation 5.

Ostendorf et al [1984] suggest that the one dimensional conservation of contaminant mass equation reduces to

$$\frac{\partial c}{\partial t} + \frac{u}{R}\frac{\partial c}{\partial x} = -\frac{\lambda c}{R} \tag{6}$$

in the absence of dispersion and far field mixing, with time t and concentration c. Equation 6 presumes that the plume and overlying uncontaminated lens travel at the same speed in the far field. The lens is somewhat lighter than the contaminated water in the plume and the density difference prevents mixing of the two fluids [Kimmel and Braids, 1980]. The uncontaminated recharge does alter the slope of the water table, however, and accordingly affects the hydraulics of the underlying plume.

The retardation factor R and decay constant λ reflect simplifying assumptions of linear adsorption and first order reaction while the neglect of dispersion is appropriate for continuous sources of pollution. We apply the chain rule to this transport equation, whence

$$\frac{dc}{dt} = \frac{\partial c}{\partial t} + \frac{\partial c}{\partial x}\,\frac{dx}{dt} \tag{7}$$

with total change dc/dt experienced in a frame of reference moving at speed dx/dt. Equations 5-7 yield the frame speed

$$\frac{dx}{dt} = \frac{u_s}{R}\left[\frac{1 + \dfrac{\varepsilon(x-x_s)}{q_s}}{1 + \dfrac{(x-x_s)\tan\beta}{h_s}}\right] \tag{8}$$

in which concentration will obey

$$\frac{dc}{dt} = -\frac{\lambda c}{R} \tag{9}$$

Ostendorf et al. [1984] integrate the latter relation from source c_s, t_s to far field c,t conditions with the result

$$c = c_s \exp\left[\frac{\lambda}{R}\,(t_s - t)\right] \tag{10}$$

The path of the moving frame follows upon integration of equation 8 from source x_s,t_s to subsequent x,t positions [Gradshteyn and Ryzhik, 1965]

$$t - t_s = \frac{Rn}{\varepsilon}\left\{(x-x_s)\tan\beta + \left(h_s - \frac{q_s\tan\beta}{\varepsilon}\right)\ln\left[1 + \frac{\varepsilon(x-x_s)}{q_s}\right]\right\} \tag{11}$$

The source conditions c_s, x_s, t_s for the far field also represent near field output conditions and link the two regions, as indicated schematically by Figure 1.

NEAR FIELD HYDRAULICS

Strong artificial recharge ε_e from the infiltration beds alters the hydraulics of the near field, where aquifer thickness is held locally constant at the value h_s and the e subscript denotes effluent conditions. The average linear velocity in the near field is taken to be a linear superposition of u_s and a radial velocity w reflecting an equivalent circular infiltration bed of radius r_e (Figure 1), centered at x = 0, y = 0, with lateral distance y. If near field time t_s dominates the hydraulic response time t_h defined by

$$t_h = \frac{\nu n x_s^2}{kgh_s} \tag{12}$$

flow will be steady, where k is permeability, ν is fluid viscosity, x_s is source location, and g is gravitational acceleration. The radial conservation of water mass becomes

$$\frac{1}{r}\frac{d(wr)}{dr} = \frac{\varepsilon_e}{nh_s} \qquad (r \leq r_e) \tag{13a}$$

$$\frac{1}{r}\frac{d(wr)}{dr} = 0 \qquad (r > r_e) \tag{13b}$$

with radial distance r and $\varepsilon_e >> \varepsilon$. Separation of variables yields a solution to equation 13

$$w = \frac{\varepsilon_e r}{2nh_s} \qquad (r \leq r_e) \tag{14a}$$

$$w = \frac{Q_e}{2\pi nh_s r} \qquad (r > r_e) \tag{14b}$$

with infiltration bed discharge Q_e defined by

$$Q_e = \pi r_e^2 \varepsilon_e \tag{15}$$

The linear superposition of ambient and radial velocities rests on the smallness of the groundwater mound amplitude H forming in response to the infiltration

$$\frac{H}{h_s} << 1 \tag{16}$$

We quantify this constraint by applying Darcy's law to the near field solution

$$w = \frac{kg}{n\nu} \frac{dn}{dr} \tag{17}$$

so that, in view of equation 14a and Figure 1, the water table depression must satisfy

$$\frac{kg}{n\nu} \frac{dn}{dr} = \frac{\varepsilon_e r}{2nh_s} \qquad (r \leq r_e) \tag{18a}$$

$$\eta = -(\eta_e + H) \qquad (r = 0) \tag{18b}$$

Integration of equation 18 by separation of variables yields

$$\frac{kg(\eta_e + H + \eta)}{\nu} = \frac{\varepsilon_e r^2}{4h_s} \qquad (r \leq r_e) \tag{19}$$

We evaluate equation 19 at $r = r_e$, where $\eta = -\eta_e$, and invoke equations 15 and 16 to deduce the near field linearity constraint

$$\frac{Q_e \nu}{4\pi kg h_s^2} << 1 \tag{20}$$

Cartesian and radial distances and velocities are related in accordance with

$$x = - r \sin\theta \tag{21a}$$

$$y = r \cos\theta \tag{21b}$$

$$u = \frac{wx}{r} \tag{21c}$$

$$v = \frac{wy}{r} \tag{21d}$$

with radial angle θ and average linear lateral velocity v as sketched in Figure 2. Recalling equation 14b, the near field velocity beyond the infiltration beds may consequently be expressed as

$$u = u_s + \frac{Q_e x}{2\pi n h_s (x^2 + y^2)} \qquad (r > r_e) \tag{22a}$$

$$v = \frac{Q_e y}{2\pi h_s n (x^2 + y^2)} \qquad (r > r_e) \tag{22b}$$

We may cast this solution in terms of a dimensionless stream function ψ [Streeter and Wylie, 1979] defined by

$$u = -u_s r_e \frac{\partial \psi}{\partial y} \tag{23a}$$

$$v = u_s r_e \frac{\partial \psi}{\partial x} \tag{23b}$$

and as such representing stream lines of the flow field. Integration of equations 22 and 23 yields [Gradshteyn and Ryzhik, 1965]

$$\psi = -\frac{y}{r_e} + \alpha \tan^{-1} \frac{x}{y} \qquad (r > r_e) \tag{24}$$

with effluent ratio α defined by

$$\alpha = \frac{Q_e}{2\pi r_e q_s} \tag{25}$$

Equations 22-25 can be verified by appropriate partial differentiation; Figure 3 displays a typical solution.

SOURCE PLANE CONDITIONS

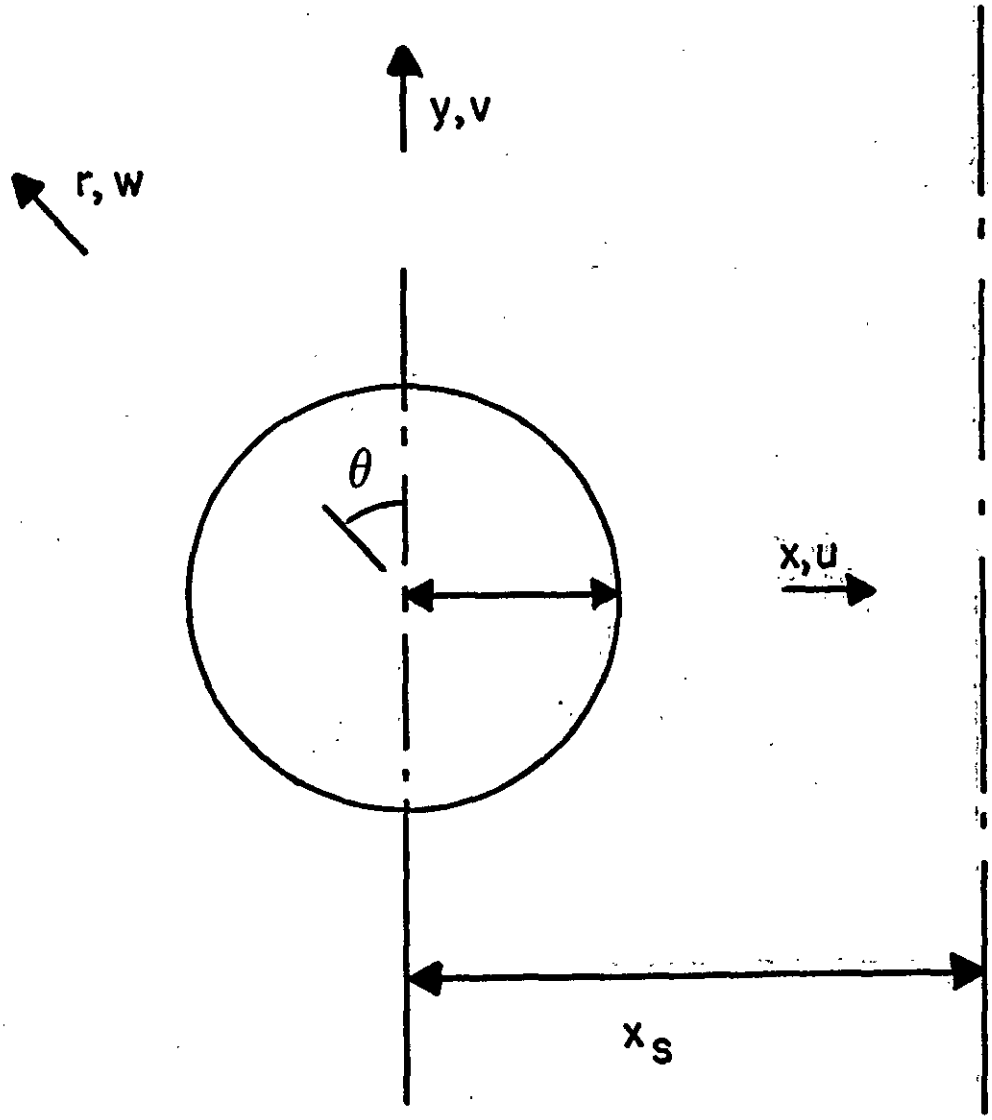

FIGURE 2 NEAR FIELD GEOMETRY

Figure 3 indicates that the largest negative stream line ψ_{max} emerging from the infiltration bed marks the lateral extent of pollution in the assumed absence of lateral mixing. ψ_{max} thus separates clean and contaminated fluid, and defines the plume in the near field. We search for this stream function by evaluating equations 21 and 24 or $r = r_e$ with the result

$$\psi = - \cos \theta - \alpha\theta \qquad (r = r_e) \qquad (26)$$

ψ_{max} follows upon zeroing of $\partial\psi/\partial\theta$ at θ_{max}

$$\theta_{max} = \sin^{-1} \alpha \qquad (0 \leq \alpha \leq 1) \qquad (27a)$$

$$\theta_{max} = \pi/2 \qquad (1 < \alpha) \qquad (27b)$$

so that, combining equations 26 and 27

$$\psi_{max} = - (1-\alpha^2)^{1/2} - \alpha \sin^{-1} \alpha \qquad (0 \leq \alpha \leq 1 \qquad (28a)$$

$$\psi_{max} = - \frac{\pi\alpha}{2} \qquad (1 < \alpha) \qquad 28b)$$

Equation 28b corresponds to the case of a strong source of infiltration, injected into the ambient flow field without dilution. All polluted stream lines emanate from the infiltration bed for this case, as indicated by Figure 3b.

The trajectory x_{max}, y_{max} of ψ_{max} corresponds to the near field boundary of the plume; in view of equation 24

$$x_{max} = y_{max} \tan \left(\frac{\psi_{max}}{\alpha} + \frac{y_{max}}{r_e \alpha} \right) \qquad (29)$$

Now we define the source plane location by an arbitrarily small lateral velocity component γu_s on ψ_{max}, i.e.

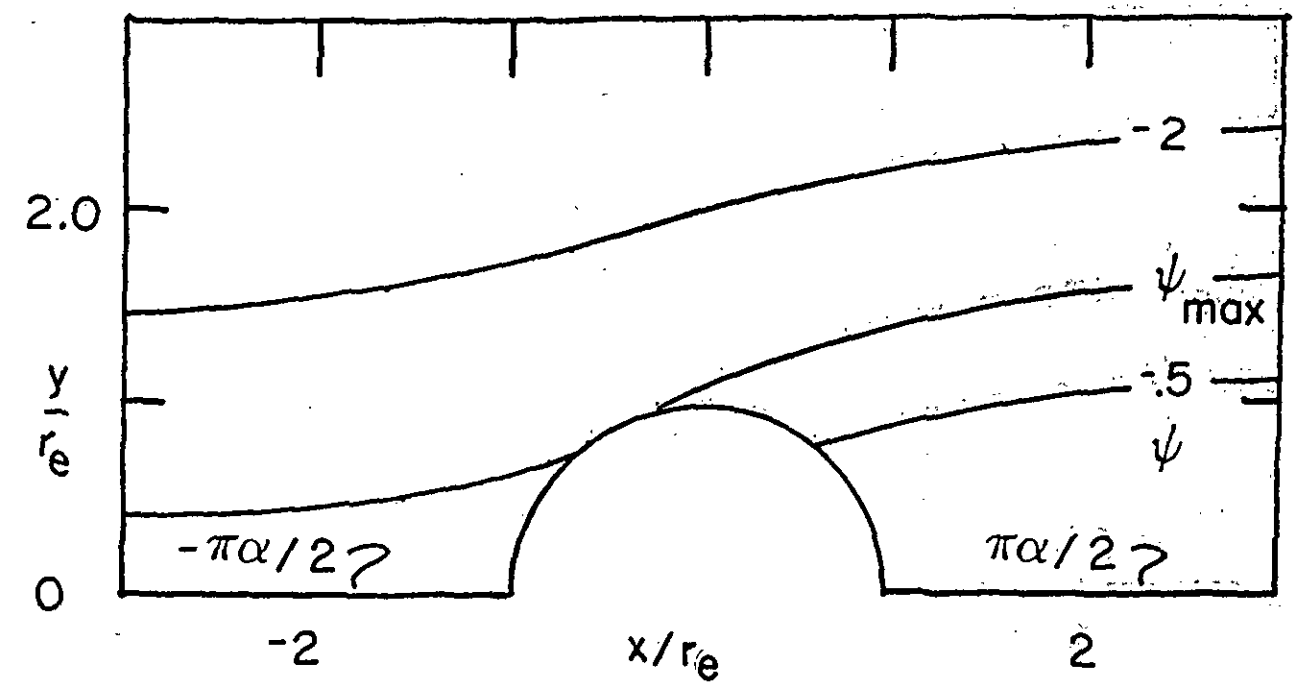

FIGURE 3a NEAR FIELD STREAM LINES FOR $\alpha = 0.5$

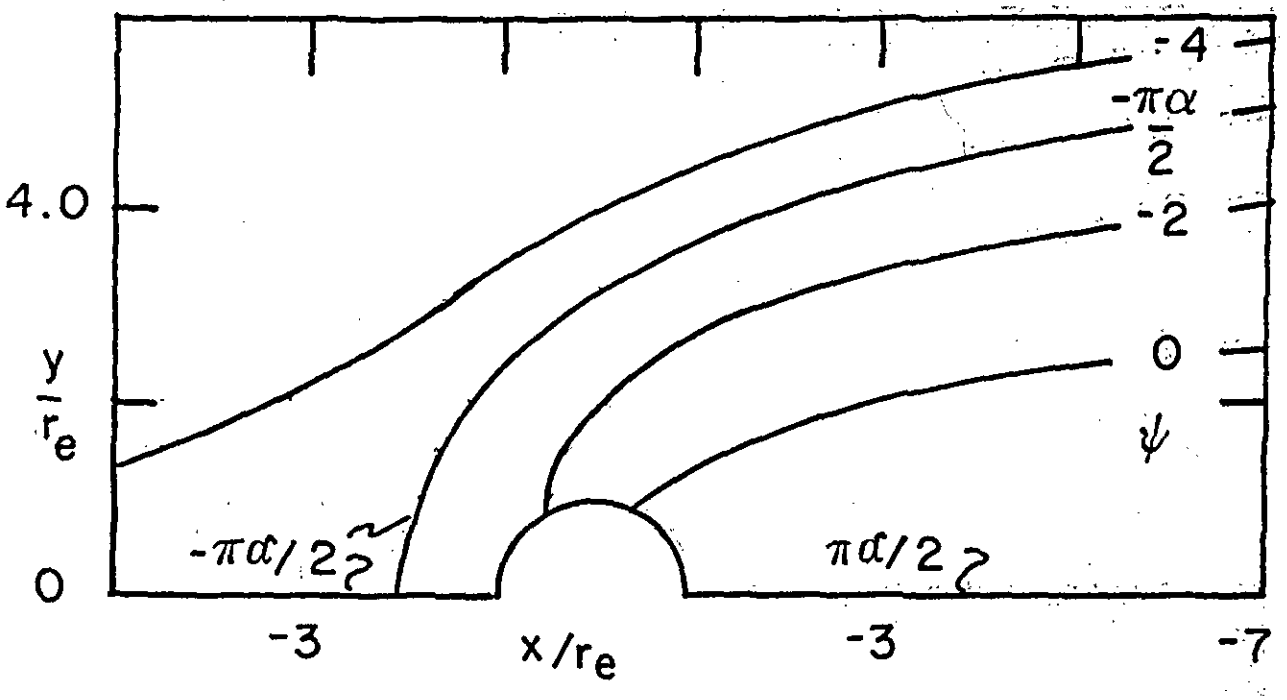

FIGURE 3b NEAR FIELD STREAM LINES FOR $\alpha = 2.0$

$$v = \gamma u_s \qquad (x_{max} = x_s,\ x_{max} > r_e,\ y_{max} = y_s) \tag{30a}$$

$$x_s = r_e \qquad (x_{max} < r_e) \tag{30b}$$

thus ensuring essentially one dimensional flow in the far field. The *Appendix* suggests that equations 22, 25, 29, and 30 yield an implicit function for the source location

$$\frac{y_s}{r_e} = -\psi_{max} + \alpha \cos^{-1}\left[\left(\frac{\gamma y_s}{\alpha r_e}\right)^{1/2}\right] \tag{31a}$$

$$\frac{x_s}{r_e} = \frac{y_s}{r_e} \tan\left(\frac{\psi_{max}}{\alpha} + \frac{y_s}{r_e \alpha}\right) \qquad (x_{max} > r_e) \tag{31b}$$

$$\frac{x_s}{r_e} = 1 \qquad (x_{max} < r_e) \tag{31c}$$

We sketch Equation 31 in Figure 4 for γ equal to 1/5.

The plume half-width b will deliver half of the total contaminated discharge Q_s through the source plane, i.e.

$$Q_s = 2bq_s \tag{32}$$

We use the stream function definition to recover Q_s as well, since it is bound by ψ_{max} and the axis of symmetry $\psi = \pi\alpha/2$ shown in Figure 3 [Streeter and Wylie, 1979]

$$Q_s = 2\left(\frac{\pi\alpha}{2} - \psi_{max}\right) u_s r_e n h_s \tag{33}$$

Equations 28 and 33 suggest that strong sources of infiltration ($\alpha > 1$) experience no dilution ($Q_s = Q_e$) in the near field, so that effluent and strong source contaminant concentrations will be equal in the absence of near field reactions. The half-width follows from equations 32 and 33

$$b = \left(\frac{\pi\alpha}{2} - \psi_{max}\right) r_e \tag{34}$$

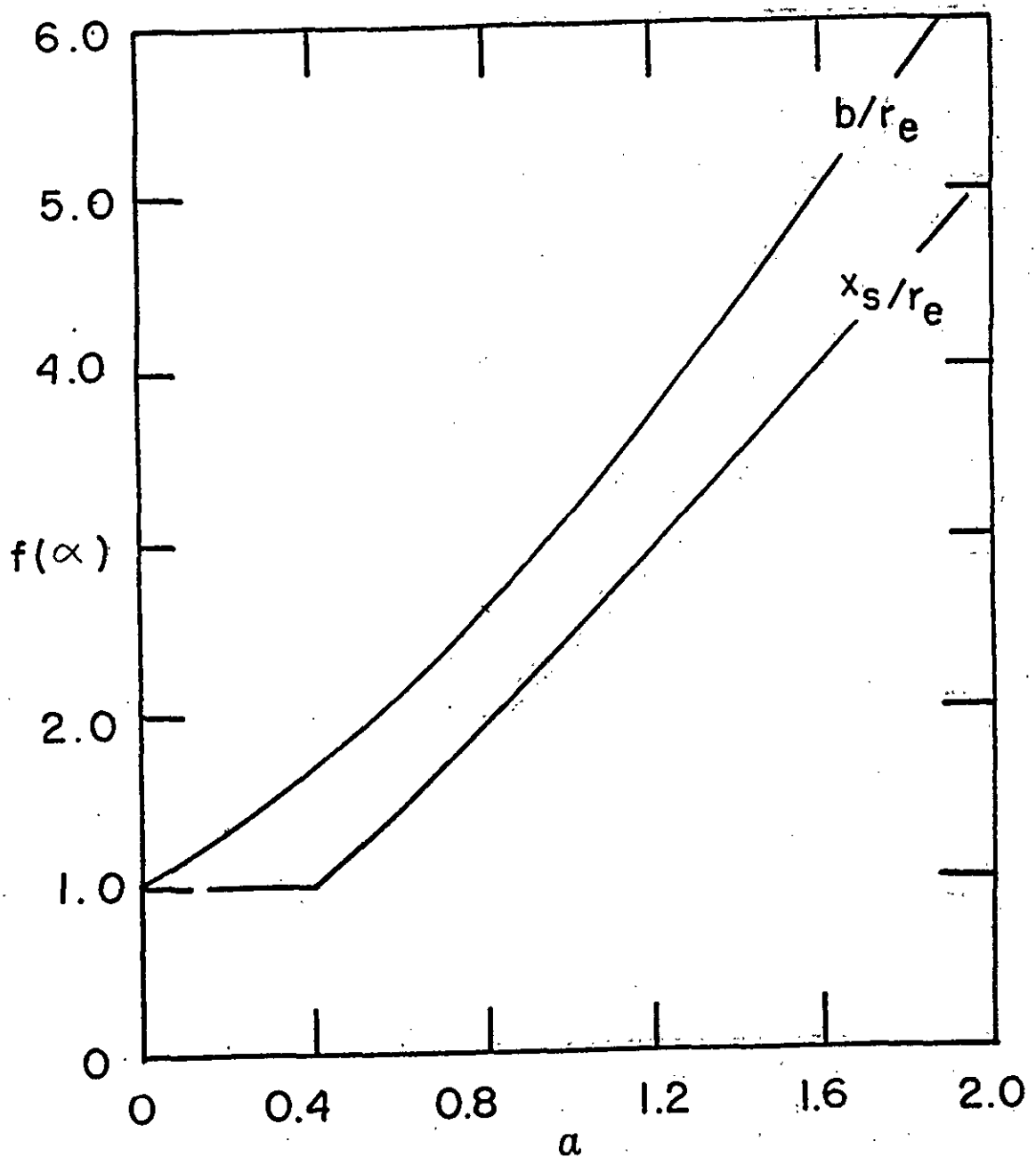

FIGURE 4 SOURCE PLANE CONFIGURATION, $\gamma = 0.2$

b will be slightly larger than y_s in magnitude; the two are equal as Y goes to zero. We also sketch equation 34 in Figure 4 to facilitate model usage.

We follow Ostendorf et al. [1984] and model the near field response to contamination as a linear system routing the vertically mixed output source plane concentration c_s in response to inputs from the infiltration bed c_e and upstream ambient flow c_a

$$Q_s c_s + RnAh_s \frac{dc_s}{dt_s} = Q_e c_e + (Q_s - Q_e)c_a \tag{35}$$

with surface area A simply estimated by

$$A = 4bx_s \tag{36}$$

Near field decay is neglected in equation 35 since the reactive time scale must dominate the near field time scale for far field concentrations to be of appreciable magnitude. The presumedly constant ambient concentration defines the excess concentration C

$$C = c - c_a \tag{37}$$

so that equations 35-37 yield a simple linear routing equation in the near field

$$\frac{dC_s}{dt_s} + \frac{C_s}{t_c} = \frac{Q_e}{Q_s} \frac{C_e}{t_c} \tag{38}$$

with near field contaminant response time t_c given by

$$t_c = \frac{2Rx_s}{u_s} \tag{39}$$

Proper neglect of near field hydraulic unsteadiness requires $t_c >> t_h$ [Gelhar and Wilson, 1974]. Equations 28, 30, 34, and 39 ensure an

asymptotic approach to the landfill source term schematization of Ostendorf et al. [1984] as α goes to zero.

We solve equation 38 for the simple case of a constant effluent concentration C_{eo} from time zero until time of shutdown t_{sd}, reflecting a change in the treatment process and a subsequent effluent concentration C_{ed}

$$C_e = C_{eo} \qquad (0 < t_s \leq t_{sd}) \qquad (40a)$$

$$C_e = C_{ed} \qquad (t_s > t_{sd}) \qquad (40b)$$

The solution to this linear, first order, nonhomogeneous, ordinary differential equation with constant coefficients is [Rainville and Bedient, 1969]

$$C_s = C_{eo} \frac{Q_e}{Q_s} \left[1-\exp\left(-\frac{t_s}{t_c}\right)\right] \qquad (0 < t_s \leq t_{sd}) \qquad (41a)$$

$$C_s = C_{ed} \frac{Q_e}{Q_s} \left[M \exp\left(-\frac{t_s}{t_c}\right) + 1\right] \quad (t_s > t_{sd}) \qquad (41b)$$

with the matching factor M defined by a continuous prediction at the time of shutdown

$$M = \left\{\frac{C_{eo}}{C_{ed}} \left[1 - \exp\left(-\frac{t_{sd}}{t_c}\right)\right] - 1 \right\} \exp\left(\frac{t_{sd}}{t_c}\right) \qquad (42)$$

c_s follows from equations 37 and 41.

OTIS AFB PLUME

We apply the foregoing theory to the observed plume generated by sewage disposal through infiltration beds at Otis Air Force Base in Barnstable County, Massachusetts, as reported by LeBlanc [1984]. The infiltration beds, starting in 1941, have discharged an average flow $Q_e = 0.0231$ m^3/sec through a bed of radius $r_e = 250$ m (half the lateral width) into a sand and

gravel aquifer of source thickness h_s = 47m, porosity $0.20 \leq n \leq 0.40$, and steep bottom slope $\tan\beta = -0.00348$. In the absence of locally definitive values for porosity, permeability, and net natural recharge, we must use the observed extent of contamination to calibrate the model hydraulics. LeBlanc [1984] measured total nitrogen N, chloride Cl, boron B, and methylene blue active substances MBAS, along with other parameters in the sewage plume. MBAS is primarily associated with synthetic detergents, first used in 1946 [LeBlanc, 1984]. The N and Cl plumes extend past the furthest downgradient observation well, while the B and MBAS plumes lie within LeBlanc's [1984] sampling domain, as suggested by Figure 5. The shorter boron plume may perhaps be attributed to adsorption onto the solid matrix [LeBlanc, 1984] and is not suitable for hydraulic calibration as a consequence. The MBAS plume, however, is not absorptive [LeBlanc, 1984]: its shorter extent is due to a later appearance of the contaminant in the effluent. By 1978, the MBAS plume extended 3700m downgradient of the infiltration beds. This observed extent calibrates the hydraulics.

A regional water table study [Guswa and LeBlanc, 1981] suggests that the natural recharge upgradient of the infiltration beds falls on a triangular area 2b by distance ℓ to the water table divide, so that mass conservation requires

$$2bq_s = \varepsilon b\ell \tag{43}$$

We substitute this equation into equation 11 to derive the arrival time t_a of the unretarded (R=1) MBAS contaminant plume, established by the reference frame starting from the source at $t_s = 0$. Solving for ε

$$\varepsilon = \frac{n}{t_a}\left\{(x_a - x_s)\tan\beta + \left(h_s - \frac{\ell\tan\beta}{2}\right)\ln\left[1 + \frac{2(x_a - x_s)}{\ell}\right]\right\} \tag{44}$$

By trial and error, with $t_a = 1.01 \times 10^9$ sec, $n = 0.30$, $x_a = 3700$m, and $\ell = 8100$m, we find $\varepsilon = 7.56 \times 10^{-9}$m/sec and $q_s = 3.06 \times 10^{-5}$ m^2/sec. The recharge estimate is lower than the natural value of 1.71×10^{-8} m/s cited by LeBlanc [1984], due possibly to domestic and public withdrawals for water supply and baseflow to surface water bodies. In any event, equations 25 and 28 yield $\alpha = 0.481$ and $\psi_{max} = -1.12$ so that, in view of Figure 4 and equation 34, the source location and plume half-width are $x_s = 294$m and $b = 468$m. The half-width compares favorably with LeBlanc's [1984] reported range of 380 to 530 m. Darcy's law and the q_s estimate specify the permeability as well

$$q_s = \frac{kgh_s}{\nu} \left(\frac{\partial n}{\partial x}\right)_s \tag{45}$$

so that, with $(\partial n/\partial x)_s = 0.0015$ and $\nu = 1.3 \times 10^{-6}$ m^2/sec, we compute $k = 5.75 \times 10^{-11} m^2$, somewhat lower than LeBlanc's [1984] value of $1.2 \times 10^{-10} m^2$ inferred from grain size distribution. The permeability estimate easily satisfies the linearity constraint of equation 20.

With the hydraulics established, contaminant transport modeling can proceed by comparing measured c_m and predicted c concentrations of Cl, MBAS, N, and B. LeBlanc [1984] reports depth varying concentrations for chloride, MBAS, and boron, while single values for total nitrogen are cited at given horizontal locations. Lateral variation of MBAS and boron are displayed as well at transects located 1020 and 2360m downgradient of the infiltration bed, while centerline concentrations only are given at 760, 2990, and 3590m

stations. The data at a given downgradient distance are all averaged arithmetically for purposes of comparison with our one dimensional model.

We compare data and theory using statistics of the error δ defined by

$$\delta = \frac{c_m - c}{c} \tag{46}$$

with mean error $\bar{\delta}$ and standard deviation σ computed in accordance with [Benjamin and Cornell, 1970]

$$\bar{\delta} = \frac{1}{j} \Sigma \delta \tag{47a}$$

$$\sigma = \left(\frac{1}{j} \Sigma \delta^2 - \bar{\delta}^2\right)^{1/2} \tag{47b}$$

The sign of $\bar{\delta}$ indicates model over or underprediction and is accordingly useful in identifying systematic model errors in the testing process: this parameter is set equal to zero in the calibration of the MBAS, N, and B predicted plumes. The error standard deviation is based on the absolute value of individuals δ's and consequently measures the magnitude of the error. In this regard, about 2/3 of our predictions lie within σ of their measured values for a zero mean error.

MODEL TESTING AND CALIBRATION

Chloride is conservative in sand and gravel aquifers [Kimmel and Braids, 1980] and may conveniently be used to test the contaminant transport model with the results summarized in Table 1 and Figure 5. Since $R = 1$ for nonadsorptive pollutants, the near field contaminant response time, in view of equation 39, is $t_c = 2.71 \times 10^8$ sec. This period dominates the near field response time $t_n = 1.3 \times 10^6$ sec implied by equation 12, so the neglect of hydraulic unsteadiness is clearly justified. LeBlanc [1984] cites recent effluent and ambient concentration data (in his Table 2) for

Table 1

Ambient and Effluent Concentrations* and Error Statistics

Contaminant	c_a	C_{eo}	C_{ed}	λ	R	$\bar{\delta}$	σ
				x 10^{-9} sec^{-1}		%	%
Cl	8.1	23.2	--	--	--	1	20
MBAS	0.0	2.10**	0.3	2.35**	--	--	27
N	0.4	21.1	--	1.69**	--	--	36
B	7	500	--	--	1.344**	--	29

*Cl, MBAS, and N concentrations in mg/ℓ, B concentrations in µg/ℓ.

**Calibrated values, MBAS λ is for biodegradable detergents.

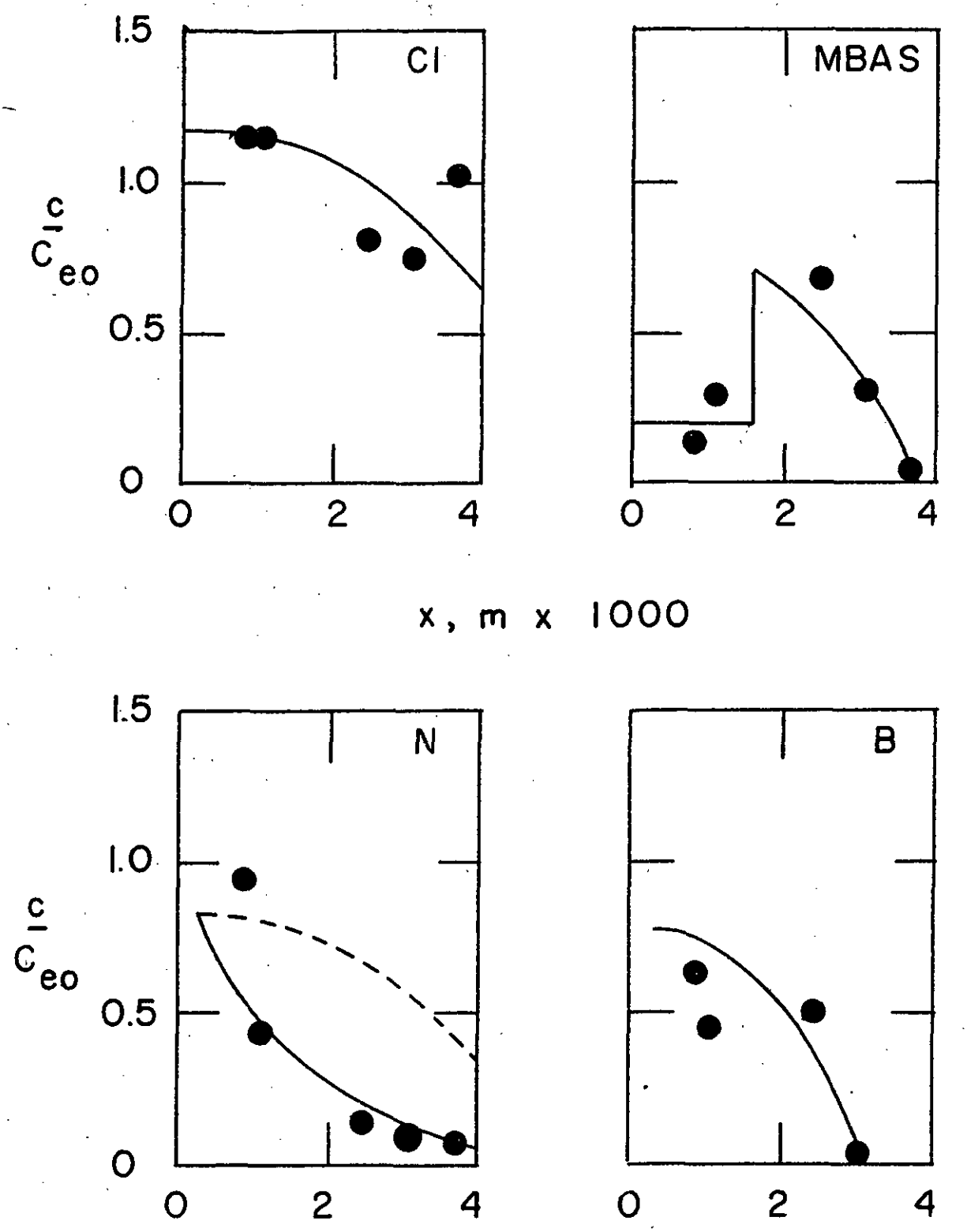

FIGURE 5. OBSERVED AND PREDICTED CONTAMINANT CONCENTRATION. DASHED N PREDICTION IS FOR CONSERVATIVE CONTAMINANT.

all four contaminants modeled, and the average values are listed in Table 1. The effluent chloride concentration in excess of ambient levels is reduced by the dilution factor Q_e/Q_s = 0.807 and routed through the near field in accordance with equations 37 and 41, which specify the source concentration c_s in a reference frame departing from the source plane at time t_s and arriving at a given far field location x in 1978. With a temporal origin set at 1941, the "present" 1978 time $t = 1.17 \times 10^9$ sec in the far field. The appropriate far field concentration c at x and t follows from equation 10: for conservative chloride $\lambda = 0$, so that c is numerically equal to the source concentration at time t_s. A sample calculation is included in the Appendix. Since R, λ, and C_{eo} are all known, the chloride comparison is a true, uncalibrated test of model accuracy. The mean error $\bar{\delta}_{Cl} = 1\%$ suggests a slight underprediction, while the 20% error standard deviation represents good model accuracy, particularly in light of the small number of sampling points and the absence of more historically definitive effluent concentration data.

The MBAS contamination is associated primarily with the use of synthetic detergents, commencing in 1946. The temporal origin for this contaminant must therefore be reset to this date, so that the 1978 far field time is 1.01×10^9 sec. Prior to 1964, the synthetic detergents were nonbiodegradable [LeBlanc, 1984] and are accordingly assumed to be conservative in our modeling efforts. Biodegradable replacements were instituted in the marketplace in 1964, however, and we assign first order reactive behavior to the subsequent MBAS source contamination. The time of shutdown $t_{sd} = 5.68 \times 10^8$ sec marks the change in postulated reaction, and

the 1978 reported effluent concentration of 0.30 mg/ℓ is taken to represent C_{ed}. Ambient MBAS levels are reported to be negligible. The initial effluent concentration is unreported, however, and we use the three observed nonbiodegradable data points, at the furthest downgradient stations, to calibrate a value of C_{eo} = 2.10 mg/ℓ. As indicated by Table 2, the C_{eo} value zeros the mean error associated with the 2360, 2990, and 3590m data. We note that the source times for these far field locations are precede the time of shutdown, so that the moving frames carry conservative, nonbiodegradable contamination. The nearest sampling points reflect more recent contamination and are used to calibrate a decay constant of 2.35 x 10^{-9} sec^{-1} for the first order biodegradation process. Figure 5 displays the observed and calibrated values, the standard deviation of 27% suggests a reasonable calibration accuracy.

Figure 5 also shows measured and conservatively computed N values, with the temporal origin once again set to 1941. The conservative concentrations, calculated in accordance with the Cl example, exceed the data with a systematic increase in error with downgradient distance; the contaminant is also found over the entire length of the conservative Cl plume. Such behavior may be explained by the postulation of a first order reaction, with the decay rate reserved as a calibration factor [Ostendorf et al., 1984]. The conservative computation is modified by incorporating a nonzero λ into equation 10, so that source and far field concentrations will differ, as indicated by Figure 5. This is also true for the biodegradable MBAS values in Table 2. A decay constant λ = 1.69 x 10^{-9} sec^{-1} zeros the mean error for total nitrogen, with a reasonable standard deviation of 36%.

Table 2

MBAS Calibration*

x	t_s	c_m	c_s	c	δ
m	sec x 10^8				%
760	8.10	0.300	0.752	0.470	-36
1020	7.10	0.650	0.978	0.483	34
2360	2.95	1.440	1.125	1.125	28
2990	1.45	0.650	0.700	0.700	-7
3590	0.21	0.100	0.120	0.120	-20

*Concentrations in mg/ℓ.

Linear adsorption exhibits a different far field behavior than first order reaction: concentrations advance at full, conservative strengths, but at a slower velocity, reflecting the retardation factor [Freeze and Cherry, 1979]. The boron plume extends to 3000 m at full strength and is thus a candidate for calibration by linear adsorption. We set the decay constant equal to zero and calibrate the observations with a modest retardation factor of R = 1.344, generating a low standard deviation of 29%. The contaminant response time, trajectory, and far field concentration equations (39, 11, and 10) must be modified to accommodate R larger than 1. The calculations are otherwise identical to the Cl example. Figure 5 again shows data and predictions. We could have obtained a similar delayed plume by postulating a later startup time for boron, as was done for MBAS. There is no historical data to support a later date, however, and LeBlanc [1984] does cite some limited evidence of adsorption for this contaminant.

CONCLUSIONS

We model the transport of a simply reactive contaminant through an infiltration bed and underlying shallow, one dimensional, unconfined aquifer with a plane, steeply sloping bottom in the assumed absence of dispersion and downgradient dilution. The effluent discharge and ambient groundwater flow under the infiltration beds are presumed to form a vertically mixed plume marked by an appreciable radial velocity component in the near field flow region. This near field analysis routes effluent contamination as a single linear reservoir whose vertically mixed output forms a source plane for the one dimensional, far field flow region downgradient of the facility; the location and width of the source plane reflects the relative strengths of ambient and effluent discharges. We model far field contaminant transport using a method of characteristics solution with frame speeds

modified by recharge, bottom slope, and linear adsorption, and concentrations reflecting first order reaction kinetics. The observed (1978) plume width downgradient of the Otis AFB sewage treatment plant in Barnstable County, Massachusetts accurately matches the predicted width, while the error standard deviation for chloride transport model testing is a reasonably low value of 20%. The accuracies are encouraging in light of the model simplicity, the lack of observed historical effluent concentrations, and the sparseness of the data base.

The MBAS, total nitrogen, and boron data illustrate three possible methods of model calibration and use. The methylene active blue substances have an unknown initial effluent concentration and the resulting "hindcasted" calibration procedure could be used to assign past responsibility for present contamination of groundwater resources. Total nitrogen concentrations are depressed below conservative values for the entire observed length of the plume. Such behavior can be simply modeled by a first order reactive mechanism, and a calibrated decay constant is put forth. The boron plume is shorter than the others, but is at full strength. This is taken to indicate linear adsorption, and a retardation factor is used to calibrate the model. The standard deviations for the three calibrations are 27, 36, and 29%, respectively, and offer further support of the model approach.

Future research may proceed on several fronts. Differential plume density may affect far field hydraulics and more realistic chemistry should be studied in an attempt to justify the calibrated constants of the Otis AFB plume. In the latter regard, total nitrogen is the expression of a coupled transport system involving ammonia, nitrate, and dissolved oxygen [Freeze and Cherry, 1979] which may yield analytical solutions in the absence of

dispersion. The relevant time scale for such a study is 10^9 secs. Such modeling efforts must remain as simple as allowed by the available data however, and we cite a continuing need for historically documented pollutant sources and spatially resolved contaminant plumes in this regard.

NOTATION

A	near field surface area, m^2.
B	boron.
b	plume half-width, m.
C	concentration above ambient, µg/ℓ or mg/ℓ.
C_{ed}	post shutdown effluent concentration above ambient, µg/ℓ or mg/ℓ.
C_{eo}	initial effluent concentration above ambient, µg/ℓ or mg/ℓ.
C_m	measured concentration above ambient, µg/ℓ or mg/ℓ.
c	concentration, µg/ℓ or mg/ℓ.
c_a	ambient concentration, µg/ℓ or mg/ℓ.
Cl	chloride.
g	gravitational acceleration m/sec^2.
H	groundwater mound amplitude, m.
h	aquifer thickness, m.
k	permeability, m^2.
ℓ	distance to water table divide, m.
M	matching factor.
MBAS	nonbiodegradable detergents.
N	total nitrogen.
n	porosity.

Q_e effluent discharge from infiltration beds, $m^3/sec.$

Q_s source plane discharge, $m^3/sec.$

q discharge per unit width, $m^2/sec.$

R retardation factor.

r radial distance, m.

r_e equivalent infiltration bed radius, m.

t far field time, sec.

t_a plume arrival time, sec.

t_c near field contaminant response time, sec.

t_h near field hydraulic response time, sec.

t_s near field time, sec.

t_{sd} time of shutdown, sec.

u average linear downgradient velocity, m/sec.

v average linear lateral velocity, m/sec.

w average linear radial velocity, m/sec.

x downgradient distance, m.

x_a plume arrival position, m.

y lateral distance, m.

α effluent ratio.

β bottom slope angle of aquifer.

γ lateral velocity ratio.

δ error.

$\bar{\delta}$ mean error.

ϵ natural recharge rate, m/sec.

ε_e effluent recharge rate from infiltration beds, m/sec.

η water table depression below source position, m.

θ radial angle.

λ decay constant, sec^{-1}.

ν fluid kinematic viscosity, m^2/sec.

σ error standard deviation.

ψ stream function.

SUBSCRIPTS

e effluent condition.

max maximum condition.

s source condition.

APPENDIX

Equations 22b and 30a ensure a small lateral velocity component on the limiting streamline ψ_{max}

$$\gamma u_s = \frac{Q_e y_s}{2\pi n h_s (x_s^2 + y_s^2)} \tag{48}$$

Since x_s and y_s lie on the streamline ψ_{max}, equation 29 holds, so that equation 48 may be expressed as

$$\gamma = \frac{\alpha r_e \cos^2\left(\frac{\psi_{max}}{\alpha} + \frac{y_{max}}{r_e \alpha}\right)}{y_s} \tag{49}$$

We invoke a equation 25 and a trigonometric identify to deduce equation 49; the implicit equation 31a follows directly from this last relation.

We illustrate the use of the contaminant transport model by predicting the chloride concentration in 1978 at a station 2360 m downgradient of the infiltration bed. All hydraulic parameters are assumed to be known: q_s, ε, h_s, tanβ, n, x_s. The equations and values describing these parameters are cited in the main text. We are interested in that frame of reference which arrives at the far field position x = 2360 m at time t = 1.17×10^8 sec, with our temporal origin set to the initiation of Cl pollution, 1941. Equation 11 suggests that this frame left the source plane at the source time $t_s = 4.52 \times 10^8$ sec. We know the source history of pollution from given values of ambient concentration, initial effluent concentration, dilution, and near field contaminant response time (c_a, C_{eo}, Q_e/Q_s, and t_c, respectively). These values, along with their defining equations, are also cited in the main text. Equations 37 and 41 yield the source concentration c_s = 23.3 mg/ℓ in force at the source plane at time t_s. Our frame will experience no change in concentration as it moves through the far field when it carries a conservative contaminant like Cl by virtue of equation 10. Thus the far field concentration c also equals 23.3 mg/ℓ, as indicated in dimensionless form by Figure 5.

REFERENCES

Bedient, P. B., Springer, N. K., Baca, E., Bouvette, T. C. Hutchins, S. R., and Tomson, M. B., Groundwater transport from wastewater infiltration, J. Environ. Eng., 109, 485-501, 1983.

Benjamin, J. R. and Cornell, C. A., Probability, Statistics and Decision for Civil Engineers, p. 12, McGraw-Hill, New York, NY, 1970.

Childs, K. E., Upchurch, S. B., and Ellis, B., Sampling of variable waste migration patterns in groundwater, Groundwater, 12, 369-376, 1974.

Finnemore, E. J. and Hantzsche, N. N., Groundwater mounding due to onsite sewage disposal, J. Irr. Drain. Eng., 109, 199-210, 1983.

Fischer, H. B., List, E. J., Koh, R. C. Y., Imberger, J., and Brooks, N. H., Mixing in Inland and Coastal Waters, pp. 10-11, Academic Press, New York, NY, 1979.

Freeze, R. A. and Cherry, J. A., Groundwater, pp. 400, 413-416, 439-440, Prentice-Hall, Englewood Cliffs, NJ, 1979.

Gelhar, L. W. and Wilson, J. L., Groundwater quality modeling, Groundwater, 12, 399-408, 1974.

Gradshteyn, I. S. and Ryzhik, I. M., Table of Integrals, Series and Products, pp. 59,60, Academic Press, New York, NY, 1965.

Guswa, J. H. and LeBlanc, D. R., Digital models of groundwater flow in the Cape Cod aquifer system, Massachusetts, USGS Open File Rept. 80-67, 1981.

Hanson, H. J. and Brock, R. R., Strip basin recharge to inclined water table, J. Hydraul. Eng., 110, 436-449, 1984.

Hantush, M. S., Growth and decay of groundwater mounds in response to uniform percolation, Water Resour. Res., 3, 227-234, 1967.

Kimmel, G. E. and Braids, O. C., Leachate plumes in groundwater from Babylon and Islip landfills, Long Island, New York, USGS Prof. Pap. 1085, 1980.

LeBlanc, D. R., Sewage plume in a sand and gravel aquifer, Cape Cod, Massachusetts, USGS Water Supply Paper 2218, 1984.

Ostendorf, D. W., Noss, R. R., and Lederer, D. O., Landfill leachate migration through shallow unconfined aquifers, Water Resour. Res., 20, 291-297, 1984.

Pinder, G. F. A Galerkin finite element simulation of groundwater contamination on Long Island, NY, Water Resour. Res., 9, 1657-1669, 1973.

Rainville, E. D. and Bedient, P. E., Elementary Differential Equations, pp. 110-125, MacMillan, New York, NY, 1969.

Streeter, V. L., and Wylie, E. B., Fluid Mechanics, pp. 313-317, McGraw-Hill, New York, NY, 1979.